Available online at www.sciencedirect.com
SCIENCE DIRECT®
Journal of Sound and Vibration 289 (2006) 595–611
JOURNAL OF SOUND AND VIBRATION
www.elsevier.com/locate/jsvi

Nonlinear free vibration behavior of functionally graded plates

J. Woo[a], S.A. Meguid[a,*], L.S. Ong[b]

[a]*Engineering Mechanics and Design Laboratory, Department of Mechanical and Industrial Engineering, University of Toronto, 5 King's College Road, Toronto, Ontario, Canada M5S 3G8*
[b]*Engineering Mechanics Division, School of Mechanical and Production Engineering, Nanyang Technological University, 50 Nanyang Avenue 639798, Singapore*

Received 4 March 2003; received in revised form 3 February 2005; accepted 15 February 2005
Available online 3 June 2005

Abstract

In this paper, an analytical solution is provided for the nonlinear free vibration behavior of plates made of functionally graded materials. The material properties of the functionally graded plates are assumed to vary continuously through the thickness, according to a power-law distribution of the volume fraction of the constituents. The fundamental equations for thin rectangular plates of functionally graded materials are obtained using the von Karman theory for large transverse deflection, and the solution is obtained in terms of mixed Fourier series. The effect of material properties, boundary conditions and thermal loading on the dynamic behavior of the plates is determined and discussed. The results reveal that nonlinear coupling effects play a major role in dictating the fundamental frequency of functionally graded plates.

1. Introduction

The concept of functionally graded materials (FGMs) was first introduced in 1984 as ultrahigh-temperature-resistant materials for aircrafts, space vehicles, nuclear and other engineering applications. Since then, FGMs have attracted much interest as heat-resistant materials. Functionally graded materials are heterogeneous composite materials, in which the material properties vary continuously from one interface to the other. This is achieved by gradually

*Corresponding author. Fax: +1 416 978 7753.
E-mail address: meguid@mie.utoronto.ca (S.A. Meguid).

0022-460X/$ - see front matter © 2005 Elsevier Ltd. All rights reserved.
doi:10.1016/j.jsv.2005.02.031

varying the volume fraction of the constituent materials. The continuity of the material properties reduces the influence of the presence of interfaces and avoids high interfacial stresses. The outcome of this is that this class of materials can survive environments with high-temperature gradients, while maintaining the desired structural integrity.

In view of these advantages, a number of investigations, dealing with thermal stresses and deformation, had been published in the scientific literature. In recent years, Tanaka et al. [1] studied an improved solution to thermoelastic material design in FGMs in order to reduce thermal stresses. Ishikawa [2] analyzed the thermal deformation and thermal stresses of FGM plates under steady graded temperature fields. Takezono et al. [3] formulated analytically and numerically the thermal stress and deformation states for axisymmetrical shells of functionally graded material subjected to thermal loading due to a fluid. Wetherhold et al. [4] considered the use of functionally graded materials to eliminate or control thermal deformation in beams and plates. Woo and Meguid [5] studied the nonlinear behavior of thin functionally graded plates and shallow shells. Considerable research has also been performed on the analysis of thermal stresses and deformation of functionally graded structures. For details and review of these studies of functionally graded materials refer to Ichikawa's works [6].

As for dynamic behavior of FGMs, Praveen and Reddy [7] investigated the response of functionally graded ceramic-metal plates using a plate finite element that accounts for transverse shear strains, rotary inertia and moderately large rotations in the von Karman sense. The static and dynamic response of the functionally graded plates was investigated by varying the volume fraction of the ceramic and metallic constituents using a simple power-law distribution. The effect of the imposed temperature field on the response of the FGM plate was also discussed. Loy et al. [8] studied the vibration of cylindrical shells of a functionally graded material made from stainless steel and nickel. The objective was to investigate the influence of the constituents' volume fractions and the configuration of the constituent materials on the natural frequency. The analysis was carried out with strain–displacement relations from Love's thin shell theory, and the eigenvalue equations were obtained using the Rayleigh–Ritz method without temperature effects.

However, studies concerning the more realistic nonlinear vibration of functionally graded plates, to our knowledge, are not found in the literature. In this work, nonlinear free vibration of functionally graded plates is studied. The governing equations for thin rectangular plates of functionally graded materials are obtained using the von Karman theory, which considers moderate deflections and small strains. The material properties of functionally graded shells are assumed to vary continuously through the thickness of the shell, according to a power-law distribution of the volume fraction of the constituents. A series solution is used to solve the coupled governing equations under simply supported, clamped and mixed boundary conditions. Numerical results are provided to show the influence of material properties, boundary conditions and thermal loading on the fundamental frequency of the plates. The advantage of the developed analysis is that the nonlinear partial differential equations can be solved directly with a semi-analytical method assuming a mixed series solution. Therefore, it can be readily used to investigate systematically the effect of various parameters including material properties, boundary conditions and thermal loading.

Following this brief introduction, we develop the fundamental equations in Section 2. The solution of the governing equations is provided in Section 3 and this is followed by numerical results and discussion of the findings in Section 4. In Section 5, we conclude this paper.

2. Fundamental equations

A rectangular plate made of FGM is considered in the present analysis. Let the xy plane of the xyz Cartesian coordinates overlap the rectangular plane area of the plate. For thin plates, the displacements are assumed to take the following form:

$$\begin{aligned} u^*(x,y,z,t) &= u(x,y,t) - zw(x,y,t)_{,x}, \\ v^*(x,y,z,t) &= v(x,y,t) - zw(x,y,t)_{,y}, \\ w^*(x,y,z,t) &= w(x,y,t), \end{aligned} \tag{1}$$

where u^*, v^* and w^* are the total displacements, and u, v and w are the middle plane displacements in the x, y and z directions, respectively.

The von Karman theory for moderately large deflections and small strains makes use of the nonlinear strain–displacement relations, in which quadratic terms in the slopes $w_{,x}$ and $w_{,y}$ are retained, while all other nonlinear terms are neglected. Therefore, the strains can be expressed as

$$\{\varepsilon\} = \begin{Bmatrix} \varepsilon_x \\ \varepsilon_y \\ \gamma_{xy} \end{Bmatrix} = \begin{Bmatrix} \varepsilon_x^0 + z\kappa_x \\ \varepsilon_y^0 + z\kappa_y \\ \gamma_{xy}^0 + z\kappa_{xy} \end{Bmatrix} \tag{2}$$

in which the middle plane strain vector $\{\varepsilon^0\}$ is given by

$$\{\varepsilon^0\} = \begin{Bmatrix} \varepsilon_x^0 \\ \varepsilon_y^0 \\ \gamma_{xy}^0 \end{Bmatrix} = \begin{Bmatrix} u_{,x} + 1/2w_{,x}^2 \\ v_{,y} + 1/2w_{,y}^2 \\ u_{,y} + v_{,x} + w_{,x}w_{,y} \end{Bmatrix} \tag{3}$$

while the curvature $\{\kappa\}$ is given by

$$\{\kappa\} = \begin{Bmatrix} \kappa_x \\ \kappa_y \\ \kappa_{xy} \end{Bmatrix} = \begin{Bmatrix} -w_{,xx} \\ -w_{,yy} \\ -2w_{,xy} \end{Bmatrix}. \tag{4}$$

The plates of the FGM are assumed to be of uniform thickness h. The material properties P of the functionally graded shells are also assumed to vary through the thickness of the plate, as a function of the volume fraction and properties of the constituent materials. These properties can be expressed as

$$P = \sum_{j=1}^{k} P_j V_j, \tag{5}$$

where P_j and V_j are the respective material property and volume fraction of the constituent material j. The volume fraction of all the constituent materials should add up to one, such that

$$\sum_{j=1}^{k} V_j = 1. \tag{6}$$

For a plate with a uniform thickness h and a reference plane at its middle plane, the volume fraction can be written as

$$V_j = \left(\frac{2z+h}{2h}\right)^n, \tag{7}$$

where n is the power-law exponent, $0 \leqslant n \leqslant \infty$. For a functionally graded solid with two constituent materials, the property variation P can be expressed as

$$P(z) = (P_u - P_l)\left(\frac{2z+h}{2h}\right)^n + P_l, \tag{8}$$

where P_u and P_l are the corresponding properties of the upper and lower planes. This power-law assumption, which is widely accepted, reflects a simple rule of mixtures used to obtain the effective properties of functionally graded materials [7]. Therefore, the material properties along the thickness of the shells, such as Young's modulus $E(z)$, Poisson's ratio $\nu(z)$, coefficient of thermal expansion $\alpha(z)$, and mass density $\rho(z)$ can be determined according to Eq. (8). With the help of these material properties, the stresses can be determined as

$$\begin{aligned}\{\sigma\} &= \begin{Bmatrix}\sigma_x\\ \sigma_y\\ \tau_{xy}\end{Bmatrix} = \frac{E(z)}{1-\nu^2(z)}\begin{bmatrix}1 & \nu(z) & 0\\ \nu(z) & 1 & 0\\ 0 & 0 & (1-\nu(z))/2\end{bmatrix}\begin{Bmatrix}\varepsilon_x\\ \varepsilon_y\\ \gamma_{xy}\end{Bmatrix} - \begin{Bmatrix}\dfrac{E(z)}{1-\nu(z)}\alpha(z)\Delta T(x,y,z)\\ \dfrac{E(z)}{1-\nu(z)}\alpha(z)\Delta T(x,y,z)\\ 0\end{Bmatrix}\\ &= [Q]\{\varepsilon\} - \begin{Bmatrix}\dfrac{E(z)}{1-\nu(z)}\alpha(z)\Delta T(x,y,z)\\ \dfrac{E(z)}{1-\nu(z)}\alpha(z\xi)\Delta T(x,y,z)\\ 0\end{Bmatrix},\end{aligned} \tag{9}$$

where $E(z)$, $\nu(z)$, $\alpha(z)$ and $\Delta T(x,y,z)$ are Young's modulus, Poisson's ratio, coefficient of linear thermal expansion and temperature referenced to the stress free state, respectively.

The axial force N and moment M can be calculated using the following expression:

$$(N_{\alpha\beta}, M_{\alpha\beta}) = \int_{-h/2}^{h/2} (1, z)\sigma_{\alpha\beta}\,\mathrm{d}z, \tag{10}$$

where α and β stand for x and y. Hence, we have

$$\begin{aligned}\{N\} &= [A]\{\varepsilon^0\} + [B]\{\kappa\} - \{N^{\mathrm{T}}\},\\ \{M\} &= [B]\{\varepsilon^0\} + [D]\{\kappa\} - \{M^{\mathrm{T}}\},\end{aligned} \tag{11}$$

in which $[A]$, $[B]$ and $[D]$ are the respective in-plane, bending–stretching coupling and bending stiffness, and are given by

$$([A],[B],[D]) = \int_{-h/2}^{h/2} (1, z, z^2)[Q]\,\mathrm{d}z \tag{12}$$

and the thermal force N^{T} and thermal moment M^{T} are given by

$$\{N^T\} = \begin{Bmatrix} N_x^T \\ N_y^T \\ 0 \end{Bmatrix} = \begin{Bmatrix} \int_{-h/2}^{h/2} \frac{E}{1-\nu}\,\alpha\Delta T\,\mathrm{d}z \\ \int_{-h/2}^{h/2} \frac{E}{1-\nu}\,\alpha\Delta T\,\mathrm{d}z \\ 0 \end{Bmatrix}, \quad \{M^{\mathrm{T}}\} = \begin{Bmatrix} M_x^T \\ M_y^T \\ 0 \end{Bmatrix} = \begin{Bmatrix} \int_{-h/2}^{h/2} \frac{E}{1-\nu}\,\alpha\Delta T z\,\mathrm{d}z \\ \int_{-h/2}^{h/2} \frac{E}{1-\nu}\,\alpha\Delta T z\,\mathrm{d}z \\ 0 \end{Bmatrix}. \tag{13}$$

If Airy's stress function φ is introduced such that

$$N_x = \varphi_{,yy}, \quad N_y = \varphi_{,xx}, \quad N_{xy} = -\varphi_{,xy} \tag{14}$$

and the unit area density of the plate is

$$\rho_0 = \int_{-h/2}^{h/2} \rho(z)\,\mathrm{d}z, \tag{15}$$

then the governing vibration equations of the plate can be reduced to

$$\begin{aligned}
&a_{22}\varphi_{,xxxx} + (2a_{12} + a_{33})\varphi_{,xxyy} + a_{11}\varphi_{,yyyy} = f_1 + f_1' - f_1^T,\\
&d_{11}w_{,xxxx} + (2d_{12} + d_{33})w_{,xxyy} + d_{22}w_{,yyyy} = q - \rho_0 w_{,tt} + f_2 + f_2' - f_2^T,\\
&f_1 = w_{,xy}^2 - w_{,xx}w_{,yy},\\
&f_1' = -[b_{12}w_{,xxxx} + (b_{11} + b_{22} - 2b_{33})w_{,xxyy} + b_{12}w_{,yyyy}],\\
&f_1^T = a_{12}N_{x,xx}^T + a_{11}N_{x,yy}^T + a_{22}N_{y,xx}^T + a_{12}N_{y,yy}^T,\\
&f_2 = \varphi_{,yy}w_{,xx} + \varphi_{,xx}w_{,yy} - 2\varphi_{,xy}w_{,xy},\\
&f_2' = c_{12}\varphi_{,xxxx} + (c_{11} + c_{22} - 2c_{33})\varphi_{,xxyy} + c_{12}\varphi_{,yyyy},\\
&f_2^T = M_{x,xx}^T + M_{y,yy}^T,\\
&[a] = [A]^{-1},\\
&[b] = [A]^{-1}[B],\\
&[c] = [B][A]^{-1},\\
&[d] = [D] - [B][A]^{-1}[B],
\end{aligned} \tag{16}$$

where f_1 and f_2 represent the effects of the von Karman nonlinear theory. The functions f_1' and f_2' represent the effect of membrane-bending coupling due to unsymmetrical material property distribution along the thickness, and f_1^T and f_2^T represent thermal loads. Only the transverse inertia force, $\rho w_{,tt}$, is considered here.

Consider now the case of a simply supported plate. In this case, the boundary conditions are

$$\begin{aligned} &x=0,a: \quad N_x=\varphi_{,yy}=0, \quad N_{xy}=-\varphi_{,xy}=0, \quad w=0, \quad M_x=0;\\ &y=0,b: \quad N_y=\varphi_{,xx}=0, \quad N_{xy}=-\varphi_{,xy}=0, \quad w=0, \quad M_y=0. \end{aligned} \tag{17}$$

While in the clamped case, the boundary conditions are represented by

$$\begin{aligned} &x=0,a: \quad N_x=\varphi_{,yy}=N_x^0, \quad N_{xy}=-\varphi_{,xy}=0, \quad w=0, \quad w_{,x}=0;\\ &y=0,b: \quad N_y=\varphi_{,xx}=N_y^0, \quad N_{xy}=-\varphi_{,xy}=0, \quad w=0, \quad w_{,y}=0. \end{aligned} \tag{18}$$

Let us now introduce the following dimensionless variables:

$$\begin{aligned} &\lambda=a/b, \quad \zeta=x/a, \quad \eta=y/b,\\ &\tau=[d_{11}/(\rho_0 a^4)]^{1/2}t,\\ &W=w/h,\\ &\Phi=\varphi/d_{11}+P(\eta^2+\rho_p\lambda^2\zeta^2)/(2\lambda^2), \quad P=-a^2N_x^0/d_{11}, \quad \rho_p=N_y^0/N_x^0,\\ &Q=a^4q/(d_{11}h),\\ &M_\zeta^T=a^2M_x^T/(d_{11}h), \quad M_\eta^T=a^2M_y^T/(d_{11}h), \quad N_\zeta^T=a^2N_x^T/(d_{11}h),\\ &N_\eta^T=a^2N_y^T/(d_{11}h),\\ &\upsilon_d=(d_{12}+2d_{33})/d_{11}, \quad \upsilon_a=(a_{12}+2a_{33})/a_{11}, \quad \upsilon_b=(b_{11}-b_{33})/b_{12},\\ &\varepsilon_b=b_{11}/h, \quad \varepsilon_a=h^2/(a_{11}d_{11}),\\ &\delta_{b12}=b_{12}/b_{11}, \quad \delta_{b33}=b_{33}/b_{11}, \quad \delta_{a12}=a_{12}/a_{11}. \end{aligned} \tag{19}$$

With the help of these dimensionless variables, the governing equations and boundary conditions become

$$\begin{aligned} &\Phi_{,\zeta\zeta\zeta\zeta}+2\upsilon_a\lambda^2\Phi_{,\zeta\zeta\eta\eta}+\lambda^4\Phi_{,\eta\eta\eta\eta}=\varepsilon_a(F_1-\varepsilon_bF_1'')-Q_N,\\ &W_{,\zeta\zeta\zeta\zeta}+2\upsilon_d\lambda^2W_{,\zeta\zeta\eta\eta}+\lambda^4W_{,\eta\eta\eta\eta}=Q-W_{,\tau\tau}+F_2+\varepsilon_bF_2''-Q_M,\\ &F_1=\lambda^2W_{,\zeta\eta}^2-\lambda^2W_{,\zeta\zeta}W_{,\eta\eta},\\ &F_1''=\delta_{b12}(W_{,\zeta\zeta\zeta\zeta}+2\upsilon_b\lambda^2W_{,\zeta\zeta\eta\eta}+\lambda^4W_{,\eta\eta\eta\eta}),\\ &Q_N=\delta_{a12}N_{\zeta,\zeta\zeta}^T+\lambda^2N_{\zeta,\eta\eta}^T+N_{\eta,\zeta\zeta}^T+\delta_{a12}N_{\eta,\eta\eta}^T,\\ &F_2=\lambda^2(\Phi_{,\eta\eta}W_{,\zeta\zeta}+\Phi_{,\zeta\zeta}W_{,\zeta\zeta}-2\Phi_{,\zeta\eta}W_{,\zeta\eta}),\\ &F_2''=\delta_{b12}(\Phi_{,\zeta\zeta\zeta\zeta}+2\upsilon_b\lambda^2\Phi_{,\zeta\zeta\eta\eta}+\lambda^4\Phi_{,\eta\eta\eta\eta}),\\ &Q_M=M_{\zeta,\zeta\zeta}^T+\lambda^2M_{\eta,\eta\eta}^T, \end{aligned} \tag{20}$$

$$\begin{aligned} \zeta=0,1: \quad &\Phi_{,\eta\eta}=0, \quad \Phi_{,\zeta\eta}=0, \quad W=0,\\ &W_{,\zeta\zeta}=\varepsilon_b[-P(1+\delta_{b12}\rho)+\delta_{b12}\Phi_{,\zeta\zeta}+N_\zeta^T+\delta_{b12}N_\eta^T]-M_\zeta^T, \end{aligned} \tag{21a}$$

$$\eta = 0, 1: \quad \Phi_{,\zeta\zeta} = 0, \quad \Phi_{,\zeta\eta} = 0, \quad W = 0,$$
$$W_{,\eta\eta} = \{\varepsilon_b[-P(\delta_{b12} + \rho) + \delta_{b12}\lambda^2\Phi_{,\zeta\zeta} + \delta_{b12}N_\zeta^T + N_\eta^T] - M_\eta^T\}/\lambda^2 \tag{21b}$$

or

$$\zeta = 0, 1: \quad \Phi_{,\eta\eta} = 0, \quad \Phi_{,\zeta\eta} = 0, \quad W = 0, \quad W_{,\zeta} = 0, \tag{22a}$$

$$\eta = 0, 1: \quad \Phi_{,\zeta\zeta} = 0, \quad \Phi_{,\zeta\eta} = 0, \quad W = 0, \quad W_{,\eta} = 0, \tag{22b}$$

which are treated in the next section.

Let us now consider the influence of a temperature field on the behavior of the composite FGM. It is assumed that one value of the temperature is imposed on the upper surface and the other value on the lower surface. This one-dimensional temperature field is assumed to be constant in the plane of the plate. In this case, the temperature distribution along the thickness can be obtained by solving a simple steady-state heat transfer equation through the thickness of the plate. The equation for the temperature through the thickness is given by

$$-(k(z)T'(z))' = 0, \tag{23}$$

where $T = T_u$ at $z = h/2$ and $T = T_l$ at $z = -h/2$. The thermal conductivity $k(z)$ is also assumed to vary according to Eq. (8). The solution to Eq. (23) is

$$T(z) = T_u - \frac{T_u - T_l}{\int_{-h/2}^{h/2} \frac{\mathrm{d}z}{k(z)}} \int_{-h/2}^{z} \frac{\mathrm{d}z}{k(z)}. \tag{24}$$

This equation does not take into consideration the temperature dependence of the material properties. As indicated in the work by Miyamoto [9], this will not have a significant effect on results. The thermal force N^{T} and thermal moment M^{T} can be calculated using Eq. (13) after the temperature field distribution has been obtained by integrating Eq. (24).

3. Solution of governing equations

Assume that a solution of W and Φ can be expressed in the following form [10]:

$$W(\zeta, \eta, \tau) = \sum_{i=0}^{I_0} W^{(i)}(\zeta, \eta) \cos \omega_i \tau,$$
$$\Phi(\zeta, \eta, \tau) = \sum_{j=0}^{J_0} \Phi^{(j)}(\zeta, \eta) \cos \omega_j \tau, \tag{25}$$

where $W^{(i)}(\zeta, \eta)$ and $\Phi^{(j)}(\zeta, \eta)$ are unknown functions of ζ and η.

Substituting Eq. (25) into Eq. (20), we obtain

$$\Phi^{(j)}_{,\zeta\zeta\zeta\zeta} + 2v_a\lambda^2\Phi^{(j)}_{,\zeta\zeta\eta\eta} + \lambda^4\Phi^{(j)}_{,\eta\eta\eta\eta} = \varepsilon_a(F_1^{(j)} - \varepsilon_b F_1'^{(j)}) - Q_N^{(j)},$$
$$W^{(i)}_{,\zeta\zeta\zeta\zeta} + 2v_d\lambda^2 W^{(i)}_{,\zeta\zeta\eta\eta} + \lambda^4 W^{(i)}_{,\eta\eta\eta\eta} = \omega_i^2 W^{(i)} + F_2^{(i)} + \varepsilon_b F_2'^{(i)} - Q_M^{(i)},$$

$$F_1^{(j)} = \frac{\lambda^2}{2}\left[\sum_{k=0}^{j}(W_{,\zeta\eta}^{(k)}W_{,\zeta\eta}^{(j-k)} - W_{,\zeta\zeta}^{(k)}W_{,\eta\eta}^{(j-k)}) + \sum_{k=j+1}^{I}(W_{,\zeta\eta}^{(k)}W_{,\zeta\eta}^{(j-k)} - W_{,\zeta\zeta}^{(k)}W_{,\eta\eta}^{(j-k)}) + \sum_{k=0}^{I}(W_{,\zeta\eta}^{(k)}W_{,\zeta\eta}^{(j+k)} - W_{,\zeta\zeta}^{(k)}W_{,\eta\eta}^{(j+k)})\right],$$

$$F_1'^{(j)} = \delta_{b12}(W_{,\zeta\zeta\zeta\zeta}^{(j)} + 2\upsilon_b\lambda^2 W_{,\zeta\zeta\eta\eta}^{(j)} + \lambda^4 W_{,\eta\eta\eta\eta}^{(j)}),$$
$$Q_N^{(j)} = \delta_{a12}N_{\zeta,\zeta\zeta}^{T(j)} + \lambda^2 N_{\zeta,\eta\eta}^{T(j)} + N_{\eta,\zeta\zeta}^{T(j)} + \delta_{a12}N_{\eta,\eta\eta}^{T(j)},$$

$$F_2^{(i)} = \frac{\lambda^2}{2}\left[\sum_{k=0}^{i}(\Phi_{,\eta\eta}^{(k)}W_{,\zeta\zeta}^{(i-k)} + \Phi_{,\zeta\zeta}^{(k)}W_{,\eta\eta}^{(i-k)} - 2\Phi_{,\zeta\eta}^{(k)}W_{,\zeta\eta}^{(i-k)}) + \sum_{k=i+1}^{J}(\Phi_{,\eta\eta}^{(k)}W_{,\zeta\zeta}^{(i-k)} + \Phi_{,\zeta\zeta}^{(k)}W_{,\eta\eta}^{(i-k)} - 2\Phi_{,\zeta\eta}^{(k)}W_{,\zeta\eta}^{(i-k)}) + \sum_{k=0}^{J}(\Phi_{,\eta\eta}^{(k)}W_{,\zeta\zeta}^{(i+k)} + \Phi_{,\zeta\zeta}^{(k)}W_{,\eta\eta}^{(i+k)} - 2\Phi_{,\zeta\eta}^{(k)}W_{,\zeta\eta}^{(i+k)})\right]$$

$$F_2'^{(i)} = \delta_{b12}(\Phi_{,\zeta\zeta\zeta\zeta}^{(i)} + 2\upsilon_b\lambda^2\Phi_{,\zeta\zeta\eta\eta}^{(i)} + \lambda^4\Phi_{,\eta\eta\eta\eta}^{(i)}),$$
$$Q_M^{(i)} = M_{\zeta,\zeta\zeta}^{T(i)} + \lambda^2 M_{\eta,\eta\eta}^{T(i)}. \tag{26}$$

Then assume that a solution of $W^{(i)}$ and $\Phi^{(j)}$ can be expressed in terms of the following series combinations:

$$W^{(i)} = \sum_{n=1}^{\infty} W_{\zeta n}^{(i)}(\zeta)\sin n\pi\eta + \sum_{m=1}^{\infty} W_{\eta m}^{(i)}(\eta)\sin m\pi\zeta + \sum_{m=1}^{\infty}\sum_{n=1}^{\infty} W_{mn}^{(i)*}\sin m\pi\zeta\sin n\pi\eta,$$
$$\Phi^{(j)} = \sum_{n=1}^{\infty} \Phi_{\zeta n}^{(j)}(\zeta)\sin n\pi\eta + \sum_{m=1}^{\infty} \Phi_{\eta m}^{(j)}(\eta)\sin m\pi\zeta + \sum_{m=1}^{\infty}\sum_{n=1}^{\infty} \Phi_{mn}^{(j)*}\sin m\pi\zeta\sin n\pi\eta, \tag{27}$$

where $W_{\zeta n}^{(i)}(\zeta)$, $W_{\eta m}^{(i)}(\eta)$, $\Phi_{\zeta n}^{(j)}(\zeta)$, $\Phi_{\eta m}^{(j)}(\eta)$ are unknown functions, and $W_{mn}^{*(i)}$, $\Phi_{mn}^{*(j)}$ are unknown constants.

Substituting Eq. (27) into Eq. (26) and expressing $Q_N^{(j)}$, $Q_M^{(i)}$, $F_1^{(j)}$, $F_1'^{(j)}$, $F_2^{(i)}$ and $F_2'^{(i)}$ in the following Fourier series form

$$Q_N^{(j)} = \sum_{m=1}^{\infty}\sum_{n=1}^{\infty} Q_{Nmn}^{(j)}\sin m\pi\zeta\sin n\pi\eta,$$
$$Q_M^{(i)} = \sum_{m=1}^{\infty}\sum_{n=1}^{\infty} Q_{Mmn}^{(i)}\sin m\pi\zeta\sin n\pi\eta,$$
$$F_1^{(j)} = \sum_{m=1}^{\infty}\sum_{n=1}^{\infty} F_{1mn}^{(j)}\sin m\pi\zeta\sin n\pi\eta,$$

$$F_1^{\prime(j)} = \sum_{m=1}^{\infty}\sum_{n=1}^{\infty} F_{1mn}^{\prime(j)} \sin m\pi\zeta \sin n\pi\eta,$$
$$F_2^{(i)} = \sum_{m=1}^{\infty}\sum_{n=1}^{\infty} F_{2mn}^{(i)} \sin m\pi\zeta \sin n\pi\eta,$$
$$F_2^{\prime(i)} = \sum_{m=1}^{\infty}\sum_{n=1}^{\infty} F_{2mn}^{\prime(i)} \sin m\pi\zeta \sin n\pi\eta, \tag{28}$$

we obtain ordinary differential equations in $W_{\zeta n}^{(i)}(\zeta)$, $W_{\eta m}^{(i)}(\eta)$, $\Phi_{\zeta n}^{(j)}(\zeta)$, $\Phi_{\eta m}^{(j)}(\eta)$ and algebraic equations in $\Phi_{mn}^{*(j)}$, $W_{mn}^{*(i)}$:

$$\frac{\mathrm{d}^4 \mathrm{W}_{\zeta n}^{(i)}(\zeta)}{\mathrm{d}^4\zeta} - 2v_d(\lambda n\pi)^2 \frac{\mathrm{d}^2 \mathrm{W}_{\zeta n}^{(i)}(\zeta)}{\mathrm{d}^2\zeta} + [(\lambda n\pi)^4 - \omega_i^2] W_{\zeta n}^{(i)}(\zeta) = 0,$$
$$\lambda^4 \frac{\mathrm{d}^4 \mathrm{W}_{\eta m}^{(i)}(\eta)}{\mathrm{d}^4\eta} - 2v_d(\lambda m\pi)^2 \frac{\mathrm{d}^2 \mathrm{W}_{\eta m}^{(i)}(\eta)}{\mathrm{d}^2\eta} + [(m\pi)^4 - \omega_i^2] W_{\eta m}^{(i)}(\eta) = 0,$$
$$[(m^2 + \lambda^2 n^2)^2\pi^4 - \omega_i^2] W_{mn}^{*(i)} = F_{2mn}^{(i)} + \varepsilon_b F_{2mn}^{\prime(i)} - Q_{Mmn}^{(i)},$$
$$\frac{\mathrm{d}^4 \Phi_{\zeta n}^{(j)}(\zeta)}{\mathrm{d}^4\zeta} - 2v_a(\lambda n\pi)^2 \frac{\mathrm{d}^2 \Phi_{\zeta n}^{(j)}(\zeta)}{\mathrm{d}^2\zeta} + (\lambda n\pi)^4 \Phi_{\zeta n}^{(j)}(\zeta) = 0,$$
$$\lambda^4 \frac{\mathrm{d}^4 \Phi_{\eta m}^{(j)}(\eta)}{\mathrm{d}^4\eta} - 2v_a(\lambda m\pi)^2 \frac{\mathrm{d}^2 \Phi_{\eta m}^{(j)}(\eta)}{\mathrm{d}^2\eta} + (m\pi)^4 \Phi_{\eta m}^{(j)}(\eta) = 0,$$
$$(m^2 + \lambda^2 n^2)^2\pi^4 \Phi_{mn}^{*(j)} = \varepsilon_a (F_{1mn}^{(j)} - \varepsilon_b F_{1mn}^{\prime(j)}) - Q_{Nmn}^{(j)}. \tag{29}$$

The solution to Eq. (29), in conjunction with some boundary conditions, can be obtained without much difficulty. If $F_{1mn}^{(j)}$, $F_{1mn}^{\prime(j)}$, $F_{2mn}^{(i)}$ and $F_{2mn}^{\prime(i)}$ are taken as constants, the solution to Eq. (29) can be obtained immediately. Once these functions as well as the constants in Eq. (27) are determined, the functions $W^{(i)}$ and $\Phi^{(j)}$ can be readily determined.

The problem is that $F_{1mn}^{(j)}$, $F_{1mn}^{\prime(j)}$, $F_{2mn}^{(i)}$ and $F_{2mn}^{\prime(i)}$ are functions of W and Φ. However, if the coefficients ω_i, $F_{2mn}^{(i)}$ and $F_{2mn}^{\prime(i)}$ are given, the function $W^{(i)}$ can be obtained by the aforementioned method. Once $F_{1mn}^{(j)}$ and $F_{1mn}^{\prime(j)}$ are determined, then $\Phi^{(j)}$ can be obtained. The thermal loads $Q_N^{(j)}$ and $Q_M^{(i)}$ are determined for a case involving transverse loads and one-dimensional temperature field. In this case, the coefficients $Q_{Nmn}^{(j)}$ and $Q_{Mmn}^{(i)}$ defined by expression (28) are determined.

At first, an initial value $W^{(i)[0]}$ is assigned to $W^{(i)}$, then the functions $F_1^{(j)}$ and $F_1^{\prime(j)}$ in Eq. (26) can be obtained and coefficients $F_{1mn}^{(j)}$ and $F_{1mn}^{\prime(j)}$ in Eq. (28) are obtained. This leads to the first approximate value $\Phi^{(j)[1]}$ of $\Phi^{(j)}$. When $W^{(i)[0]}$ and $\Phi^{(j)[1]}$ are determined, functions $F_2^{(j)}$ and $F_2^{\prime(j)}$ in Eq. (26) can be obtained, and then the first approximate value $W^{(i)[1]}$ of $W^{(i)}$ can be determined. This is continued until we develop a series of approximate solutions for $W^{(i)[1]}$, $\Phi^{(j)[1]}$; $W^{(i)[2]}$, $\Phi^{(j)[2]}$; …; $W^{(i)[n-1]}$, $\Phi^{(j)[n-1]}$); $W^{(i)[n]}$, $\Phi^{(j)[1]}$ by the nth iteration. If the difference between the solutions of the $(n-1)$th and nth is within an assumed tolerance of 10^{-4}, we accept the values of $W^{(i)}$ and $\Phi^{(j)}$ as the solution.

When the plate vibrates at the frequency ω_i that is approaching the natural frequency of the plate, resonance will occur. Under such circumstances, the equations given by Eq. (29) become singular. In order to obtain the frequency–amplitude relations in this case, we prescribe one of the coefficients $W_{mn}^{*(i)}$ of the function $W^{(i)}$ first; then, the other coefficients $W_{mn}^{*(i)}$ and the frequency ω_i can thus be determined. The particular $W_{mn}^{*(i)}$ whose value is prescribed is chosen in accordance with the vibration mode of the plates. In the case of simply supported or clamped square plates that vibrate into one half-wave in both ζ and η directions, the coefficient $W_{11}^{*(i)}$ is dominant. For a very small value of $W_{11}^{*(i)}$, for example of $W_{11}^{*(i)} = 10^{-5}$, the corresponding value of ω_i may be taken to be the natural frequency of the plate. Once these functions and constants are determined, the solution to the nonlinear equations (26) that govern the plate vibration can be obtained.

4. Numerical results and discussion

The number of I_0 and J_0 terms in series expansion in $\cos \omega_i \tau$ is tried to obtain an appropriate solution. For the cases of $I_0 = 1$, $J_0 = 2$ and $I_0 = 2$, $J_0 = 4$, the difference of results is negligible. Therefore, for the sake of convenience, we select $I_0 = 1$, $J_0 = 2$ in our analysis.

The solution of Eq. (26) was carried out using M_0 and N_0 terms in the Fourier series. The number of terms M_0 and N_0 needed for convergence was carefully examined (Fig. 1) for a simply supported square aluminum–zirconia plate ($n = 1$). The maximum difference between $M_0 = N_0 = 5$ and $M_0 = N_0 = 7$ is 0.4%, and between $M_0 = N_0 = 7$ and $M_0 = N_0 = 9$ is less than 0.1%. Therefore, $M_0 = N_0 = 7$ was used for all subsequent analyses. This is also in agreement with our earlier work [5].

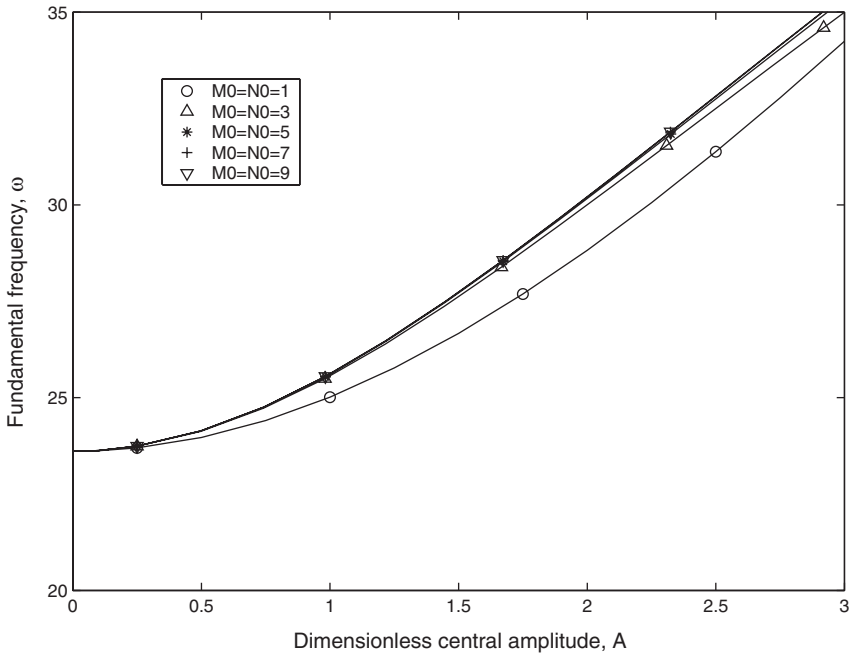

Fig. 1. Convergence of ω with M_0 and N_0 terms in the Fourier series for a simply supported square aluminum–zirconia plate ($n = 1$) : ◯, $M_0 = N_0 = 1$; △, $M_0 = N_0 = 3$; +, $M_0 = N_0 = 5$; ∗, $M_0 = N_0 = 7$; ▽, $M_0 = N_0 = 9$.

The analytic results are presented in terms of dimensionless deflection and frequency. The dimensionless parameters used are as follows:

Center deflection $W = w/h$,

Load parameter $P = -N_x^0 a^2/(E_m h^3)$,

Thickness coordinate $Z = z/h$,

Time $\tau = \{E_m h^3/[12(1-\nu_m^2)\rho_m a^4]\}^{1/2} t$,

where E_m, ν_m, ρ_m are Young's modulus, Poisson's ratio and density of the metal used in the functionally graded material, respectively. N_x^0 is a uniformly distributed axial load acting along the edges $x = 0$ and $x = a$, a is the length of the plate and h is the thickness of that plate. The analysis was performed on a square plate of side $a = b = 0.2\,m$ and thickness $h = 0.01\,m$.

Four cases of boundary conditions are examined, as summarized in Table 1.

The analysis of the FG plates was conducted for two types of ceramic and metal combinations. The first set of materials considered was zirconia and aluminum. The second one was a combination of alumina and aluminum. Table 2 details the material properties. In all cases, the lower surface of the shell is assumed to be metal (aluminum) rich and the upper surface is assumed to be pure ceramic (alumina or zirconia). In this analysis, only nonlinear elastic behavior of the FG plates was considered.

Fig. 2 shows the relation of the central amplitude of vibration and fundamental frequency for four simply supported square aluminum–zirconia plates. It is noted that the fundamental frequency of the plate increases with the amplitude of vibration. This is due to the fact that the in-plane axial force in the plate contributes to the lateral stiffness resulting from nonlinear coupling.

Table 1
Four cases of boundary conditions under investigation

Case	Boundary	$\zeta = 0$	$\zeta = 1$	$\eta = 0$	$\eta = 1$
I	All edges clamped	$W = W_{,\zeta} = 0$	$W = W_{,\zeta} = 0$	$W = W_{,\eta} = 0$	$W = W_{,\eta} = 0$
II	All edges simply supported	$W = M_\zeta = 0$	$W = M_\zeta = 0$	$W = M_\eta = 0$	$W = M_\eta = 0$
III	Two opposite edges simply supported and others clamped	$W = M_\zeta = 0$	$W = M_\zeta = 0$	$W = W_{,\eta} = 0$	$W = W_{,\eta} = 0$
IV	Two adjoining edges simply supported and others clamped	$W = M_\zeta = 0$	$W = W_{,\zeta} = 0$	$W = M_\eta = 0$	$W = W_{,\eta} = 0$

Table 2
Material properties

Materials	Young's modulus (GPa)	Poisson's ratio	Density (kg/m^3)	Thermal conductivity (W/mK)	Coefficient of thermal expansion ($\times 10^{-6}/^\circ$C)
Aluminum	70	0.3	2707	204	23.0
Alumina	380	0.3	3800	10.4	7.4
Zirconia	151	0.3	3000	2.09	10.0

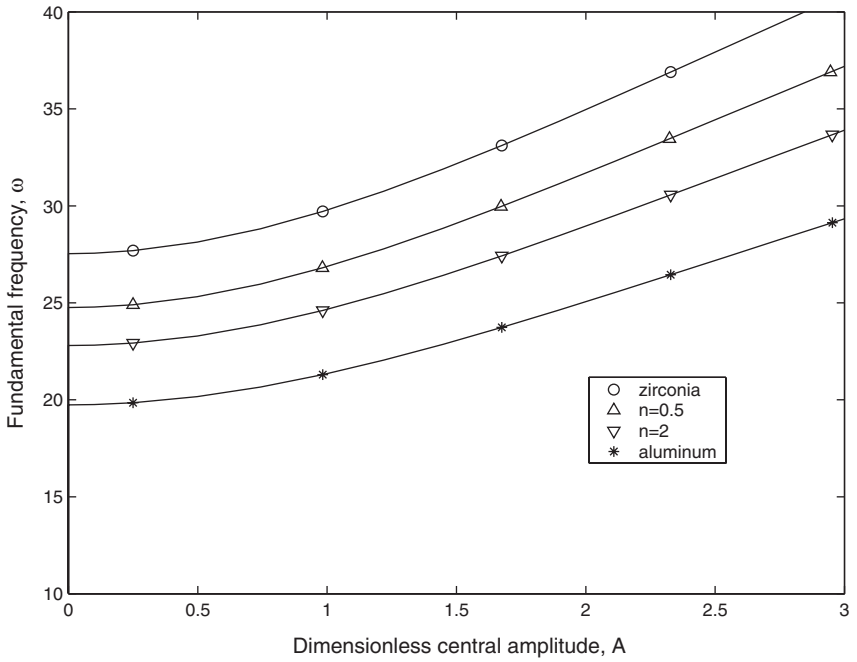

Fig. 2. The central amplitude of vibration versus fundamental frequency for four simply supported square aluminum–zirconia plates: ◯, zirconia; △, $n = 0.5$; ▽, $n = 2.0$; ∗, aluminum.

This indicates that the fundamental frequency depends upon the amplitude of vibration, which is significantly different from the linear dynamic response.

Let us now consider the influence of a temperature field on the behavior of the functionally graded composite. In the present analysis, we assume the plate is subjected to a one-dimensional temperature field, where the lower surface was held at a prescribed temperature of 20 °C and the upper surface at 600 °C, so the temperature difference (ΔT) between the top and bottom surface is 580 °C. The initial stress-free state is assumed to exist at a temperature of $T_0 = 0\,^{\circ}\mathrm{C}$. Fig. 3 shows the temperature distribution through the thickness of the aluminum–zirconia plates for various values of the volume fraction exponent n. Now that the temperature field distribution is obtained, the thermal force N^{T} and thermal moment M^{T} can be calculated using Eq. (13). The solution of the coupled equations governing the vibration behavior of the FGM plate given by Eq. (20) under a temperature field can also be obtained using the aforementioned method.

The relation of the central amplitude of vibration and fundamental frequency for four simply supported square aluminum–zirconia plates subjected to the prescribed temperature field is shown in Fig. 4. The existence of the temperature increases the fundamental frequency of the plates. This is due to thermal deflection of the plates. However, the influence of this deflection decreases rapidly with the increase in the amplitude of vibration. The effect of the temperature field on the fundamental frequency of the pure aluminum and zirconia plates is more pronounced than that of the aluminum–zirconia plates. As can be seen in Fig. 4, the maximum variation of the fundamental frequency due to the temperature field for FG plates was found to be only 0.8%. As such, it can be argued that the existence of the temperature field does not play a major role in such a situation.

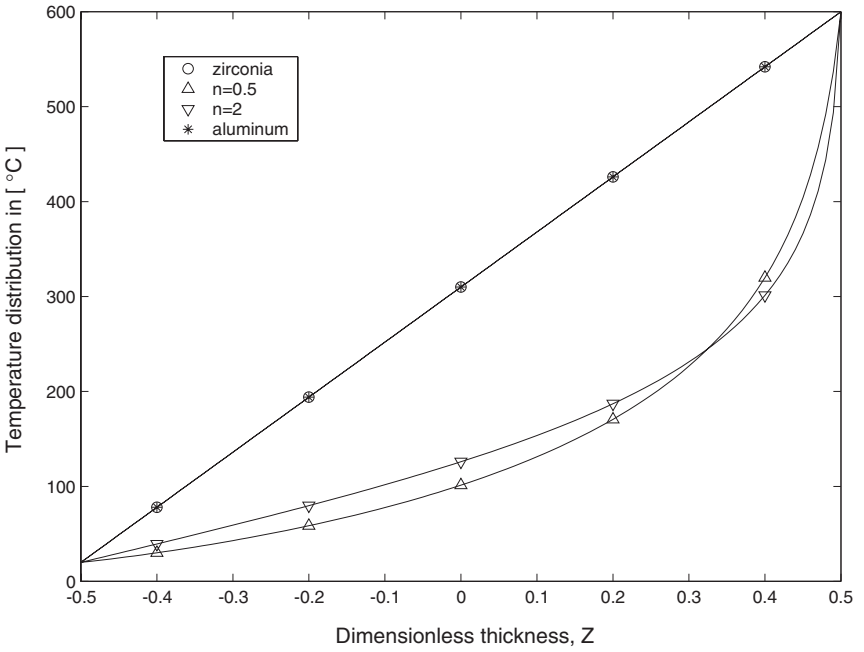

Fig. 3. Temperature field through the thickness of the FGM plates (aluminum–zirconia): ◯, zirconia; △, $n = 0.5$; ▽, $n = 2.0$; ∗, aluminum.

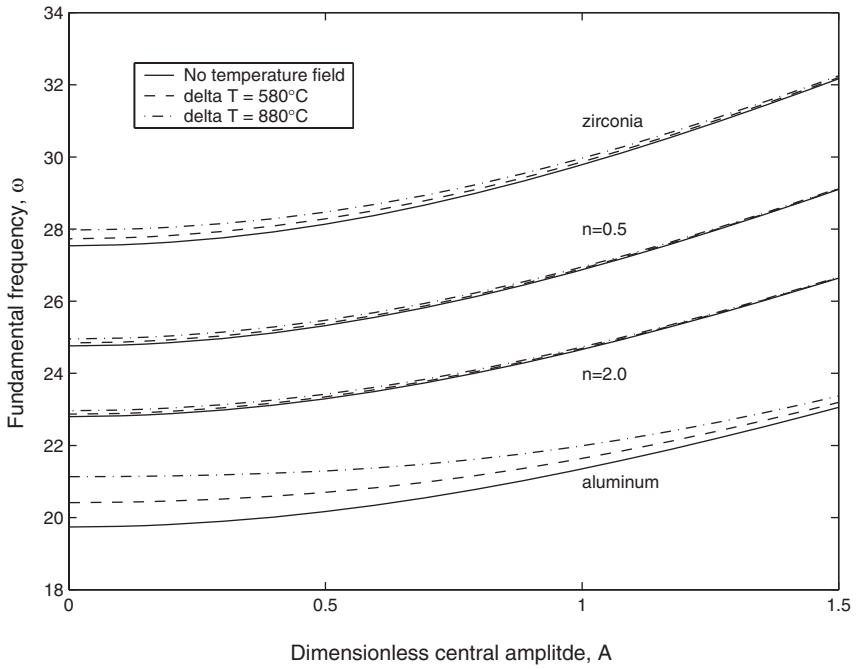

Fig. 4. The central amplitude of vibration versus fundamental frequency for four simply supported square aluminum–zirconia plates and the effect of the temperature fields: ——, no temperature field; - - - -, $\Delta T = 580\,^{\circ}\mathrm{C}$; –·–·–, $\Delta T = 880\,^{\circ}\mathrm{C}$.

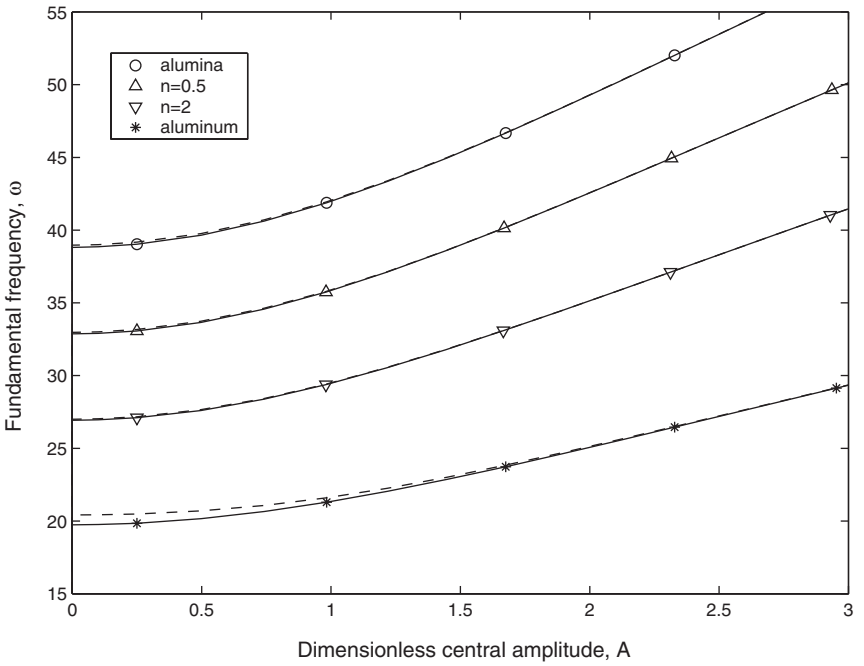

Fig. 5. The central amplitude of vibration versus fundamental frequency for four simply supported square aluminum–alumina plates and the effect of the temperature field (dashed line): ◯, alumina; △, $n = 0.5$; ▽, $n = 2.0$; ∗, aluminum.

Fig. 5 shows the variation of the normalized central amplitude of vibration and the fundamental frequency for four simply supported square aluminum–alumina plates. The higher fundamental frequency exhibited by the plates in this case is due to the higher Young's modulus E of the alumina.

Fig. 6 shows the variation of the central amplitude of vibration and fundamental frequency for square aluminum–zirconia plates with the two opposite edges being simply supported and the other edges being clamped (case III). Fig. 7 shows the variation of the central amplitude of vibration and fundamental frequency for square aluminum–zirconia plates with two adjoining edges simply supported and the other edges clamped (case IV). In these two cases, we find that the temperature field plays an insignificant role in the fundamental frequency of the plates.

Fig. 8 depicts the variation of the central amplitude of vibration and the fundamental frequency for four clamped square aluminum–zirconia plates. It is worth noting that the existence of the temperature field does not affect the fundamental frequency of the plates at all, since the clamped boundary condition (case I) does not exhibit lateral thermal deflection. Under such a circumstance, the central amplitude of vibration and fundamental frequency are unaffected by the temperature field.

Fig. 9 shows the relation of the central amplitude of vibration and fundamental frequency for a clamped square aluminum–zirconia plate ($n = 1$) with different levels of edge compression ($+P$) or tension ($-P$). Note that P is the critical compression under which the plate will buckle without vibration. The existence of a compressive edge loading reduces the fundamental frequency of the plate due to the weakening effect of the pre-stress. Conversely, a tensile edge load (such as $-0.5P$) increases the fundamental frequency due to the stiffening effect.

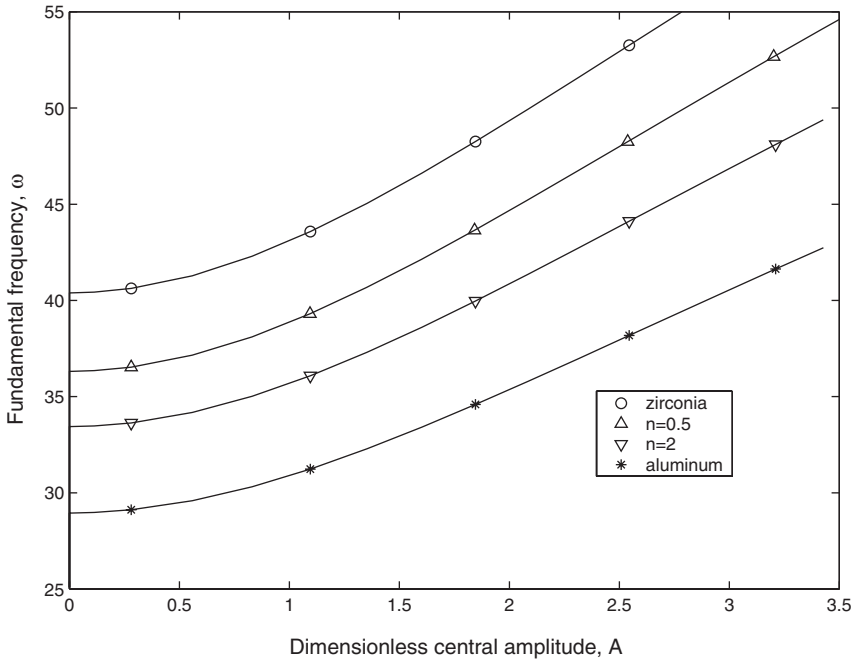

Fig. 6. The central amplitude of vibration versus fundamental frequency for square aluminum–zirconia plates with two opposite edges simply supported and the other edges clamped (case III): ◯, zirconia; △, $n = 0.5$; ▽, $n = 2.0$; ∗, aluminum.

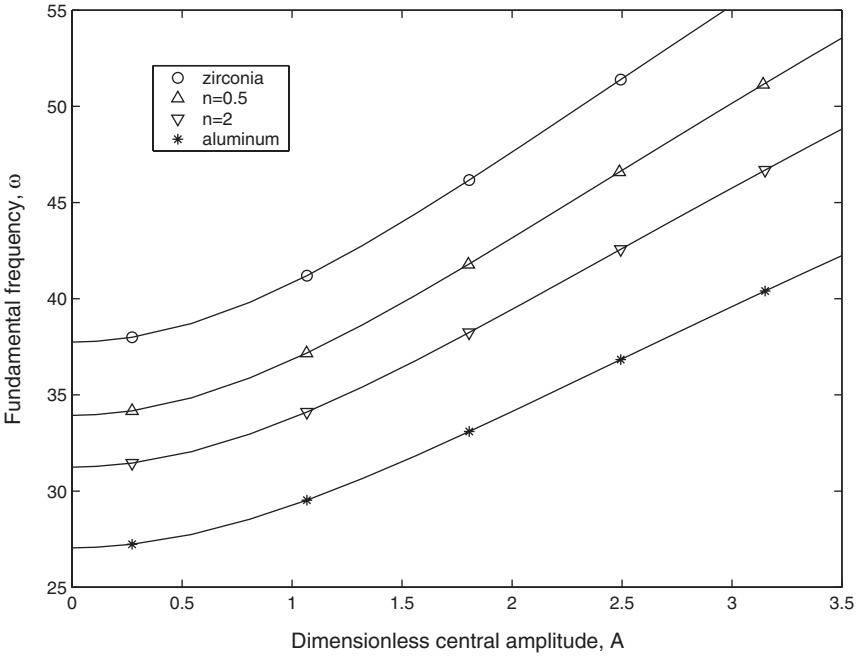

Fig. 7. The central amplitude of vibration versus fundamental frequency for square aluminum–zirconia plates with two adjoining edges simply supported and the other edges clamped (case IV): ◯, zirconia; △, $n = 0.5$; ▽, $n = 2.0$; ∗, aluminum.

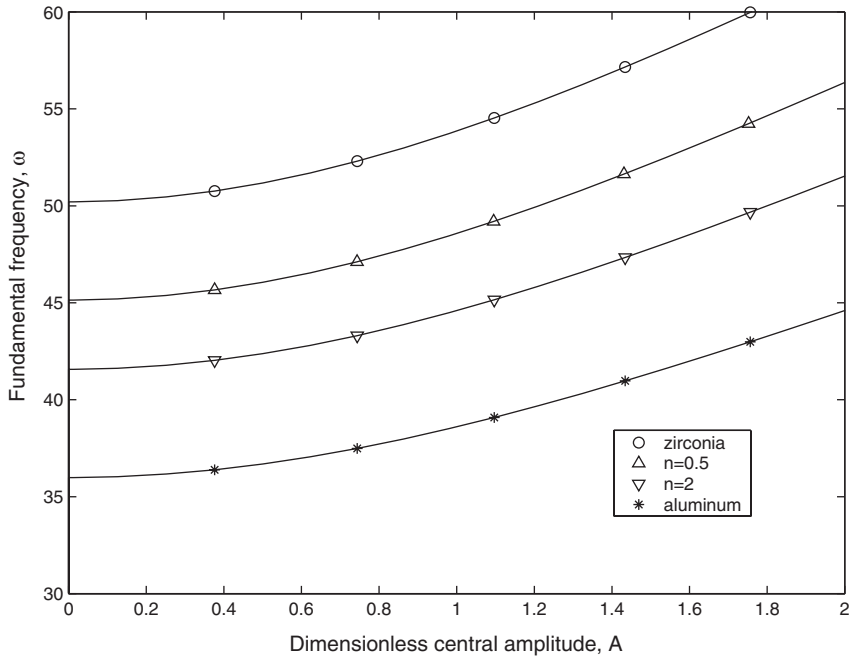

Fig. 8. The central amplitude of vibration versus fundamental frequency for four clamped square aluminum–zirconia plates: ◯, zirconia; △, $n = 0.5$; ▽, $n = 2.0$; ∗, aluminum.

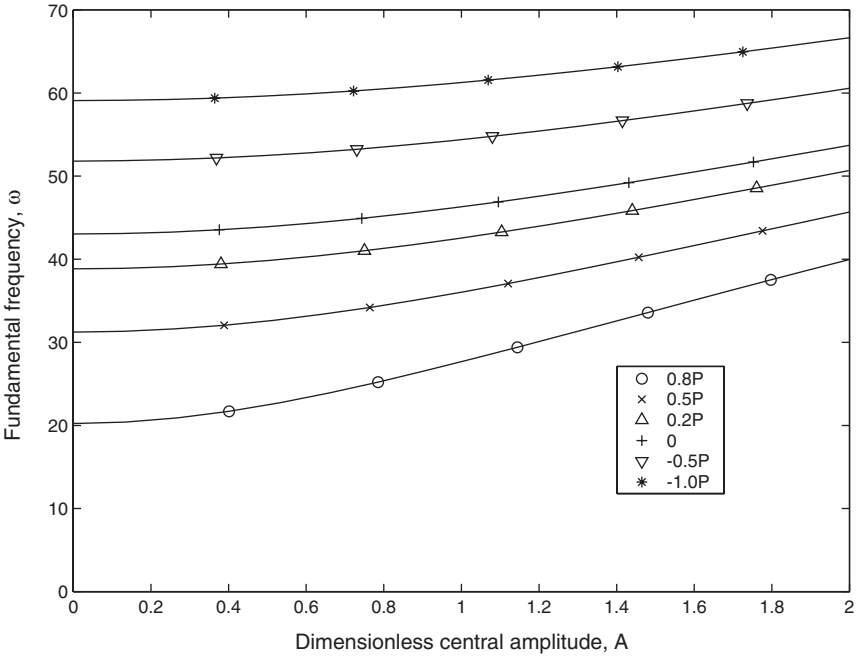

Fig. 9. The central amplitude of vibration versus fundamental frequency for a clamped square aluminum–zirconia plate ($n = 1$) with different edge compressions or tensions: ◯, $0.8P$; ×, $0.5P$; △, $0.2P$; +, 0; ▽, $-0.5P$; ∗, $-1.0P$.

5. Conclusion

The nonlinear free vibration behavior of plates made of functionally graded materials is studied. The fundamental equations for plates made of FGM have been obtained using the von Karman theory for large transverse deflections. The material properties of FGM shells are assumed to vary continuously through the thickness of the shell, and were graded according to a power-law distribution of the volume fraction of the constituents. The advantage of the developed analysis is that the nonlinear partial differential equations can be solved directly with a semi-analytical method assuming a mixed series solution. Therefore, it can be readily used to investigate systematically the effect of various parameters including material properties, boundary conditions and thermal loading on the behavior of the plate due to this advantage. The results reveal that nonlinear coupling effects play a major role in dictating the response of the functionally graded plates. Specifically, the results reveal that

(a) the fundamental frequency increases with the amplitude of vibration of the FGM plates due to nonlinear coupling between bending and in-plane stretching,
(b) the existence of the temperature field increases the fundamental frequency of the FGM plates with simply supported edges, but the temperature field does not affect the fundamental frequency of the plates with all edges being clamped, and
(c) the existence of the temperature field does not play a major role in increasing the fundamental frequency of the FGM plates.

References

[1] K. Tanaka, Y. Tanaka, H. Watanabe, V.F. Poterasu, Y. Sugano, Improved solution to thermoelastic material design in functionally graded materials: scheme to reduce thermal stresses, *Computer Methods in Applied Mechanics and Engineering* 109 (1993) 377–389.
[2] T. Ishikawa, Thermal deformation and thermal stress of FGM plates under steady graded temperature field, in: *Proceedings of the First International Symposium on FGM*, Sendai, Japan, 1990, pp. 11–25.
[3] S. Takezono, K. Tao, E. Inamura, M. Inoue, Thermal stress and deformation in functionally graded material shells of revolution under thermal loading due to fluid, *JSME International Journal Series A: Mechanics and Material Engineering* 39 (1996) 573–581.
[4] R.C. Wetherhold, S. Seelman, J. Wang, Use of functionally graded materials to eliminate or control thermal deformation, *Composites Science and Technology* 56 (1996) 1099–1104.
[5] J. Woo, S.A. Meguid, Nonlinear behaviour of functionally graded plates and shallow shells, *International Journal of Solids and Structures* 38 (2001) 7409–7421.
[6] K. Ichikawa, *Functional Graded Materials in the 21st Century*, Kluwer Academic Publishers, Norwell, MA, 2000.
[7] G.V. Praveen, J.N. Reddy, Nonlinear transient thermoelastic analysis of functionally graded ceramic-metal plates, *International Journal of Solids and Structures* 35 (1998) 4457–4476.
[8] C.T. Loy, J.N. Lam, J.N. Reddy, Vibration of functionally graded cylindrical shells, *International Journal of Mechanical Science* 41 (1999) 309–324.
[9] Y. Miyamoto, *Functional Graded Materials: Design, Processing and Applications*, Kluwer Academic Publishers, Boston, MA, 1999.
[10] A.H. Nayfeh, D.T. Mook, *Nonlinear Oscillations*, Wiley, New York, 1979.